

# Cannabinoid type 1 receptor blockade induces transdifferentiation towards a brown fat phenotype in white adipocytes

N. Perwitz<sup>1</sup>, J. Wenzel<sup>2</sup>, I. Wagner<sup>1</sup>, J. Büning<sup>1</sup>, M. Drenckhan<sup>1</sup>, K. Zarse<sup>3</sup>, M. Ristow<sup>3</sup>, W. Lilienthal<sup>4</sup>, H. Lehnert<sup>1</sup> & J. Klein<sup>1</sup>

<sup>1</sup>Department of Internal Medicine I, University of Luebeck, Germany

<sup>2</sup>Institute of Experimental and Clinical Pharmacology and Toxicology, University of Luebeck, Germany

<sup>3</sup>Department of Human Nutrition, Institute of Nutrition, Friedrich-Schiller-University of Jena, Germany

<sup>4</sup>Sanofi-Aventis Deutschland GmbH, Berlin, Germany

**Aim:** The endocannabinoid (EC) system is a major component in the control of energy homeostasis. It mediates a positive energy balance via central and peripheral pathways. Blockade of the cannabinoid type 1 receptor induces weight reduction and improves cardiovascular risk factors in overweight patients. Cannabinoid receptor type 1 (CB1R)-deficient mice are resistant to diet-induced obesity. The mechanisms responsible for these effects remain only partially elucidated. We hypothesized peripheral effects via direct modulation of adipocyte function to be an integral part of EC action on energy metabolism and insulin sensitivity.

**Methods:** SV40 immortalized murine white and brown adipocytes were used for all experiments. We investigated the effect of CB1R blockade by stimulating the cells acutely and chronically with rimonabant, a selective antagonist for the CB1R, or by knocking down the receptor with small interfering RNA (siRNA). Changes in thermogenic mRNA and protein expression as well as mitochondrial biogenesis and function were assessed by real-time RT-PCR, immunoblotting, fluorescent staining techniques, electron microscopy and by measuring oxygen consumption.

**Results:** Acute and chronic blockade of the CB1R with the selective antagonist rimonabant or by siRNA in murine white adipocytes strongly induced the thermogenic uncoupling protein-1 (UCP-1). UCP-1 expression was increased in a time- and dose-dependent manner both at the RNA and protein level. Furthermore, this effect was paralleled by enhanced peroxisome proliferator-activated receptor  $\gamma$  coactivator 1 $\alpha$  (PGC-1 $\alpha$ ) expression. In accordance with these findings, AMP-activated protein kinase (AMPK) phosphorylation was also increased after rimonabant treatment. Mitochondria-specific fluorescent staining demonstrated an augmentation in the number of mitochondria. This was confirmed by electron microscopy images. Moreover, rimonabant treatment enhanced the cytochrome c oxidase activity and increased cellular oxygen consumption.

**Conclusions:** Taken together, our data demonstrate that inhibition of peripheral CB1R action in adipocytes directly promotes transdifferentiation of white adipocytes into a mitochondria-rich, thermogenic brown fat phenotype. Enhanced thermogenesis and insulin sensitivity may represent a peripheral mechanism contributing to weight loss and improved glucose homeostasis in rimonabant-treated patients.

**Keywords:** adipocyte, endocannabinoid action, mitochondrial biogenesis, oxygen consumption, transdifferentiation, uncoupling protein 1

Received 13 February 2009; returned for revision 15 July 2009; revised version accepted 15 July 2009

## Introduction

Obesity is a result of an imbalance between energy intake and energy expenditure. It is characterized by an increase in total white fat mass. Alteration of adipocyte function is a critical component in the pathogenesis of obesity and its related cardiometabolic complications. There are two different types of fat cells. Whereas white fat is responsible for energy storage, brown adipose tissue dissipates energy by uncoupling oxidative phosphorylation from ATP production, a process mediated

by the mitochondrial uncoupling protein-1 (UCP-1). UCP-1 expression, in turn, is critically regulated by the transcriptional peroxisome proliferator-activated receptor  $\gamma$  coactivator 1 $\alpha$  (PGC-1 $\alpha$ ), which increases the transcriptional activity of peroxisome proliferator-activated receptor  $\gamma$  (PPAR $\gamma$ ) on the UCP-1 promoter [1]. Ectopic expression of PGC-1 $\alpha$  in white adipose cells activates expression of UCP-1 and key mitochondrial enzymes of the respiratory chain and also enhances the cellular mitochondrial DNA [2]. PGC-1 $\alpha$  promotes a metabolic shift in white fat cells that form lipid storage towards fatty acid utilization [3].

The endocannabinoid system is a critical component in the control of energy metabolism [4]. Stimulation of the cannabinoid receptor type 1 (CB1R) with a specific agonist

Correspondence to: J. Klein, Department of Internal Medicine I, University of Luebeck, Ratzeburger Allee 160, 23538 Luebeck, Germany.  
E-mail: j.klein@uni-luebeck.de

WIN 55212.2 has a negative impact on thermogenesis in brown adipocytes and further favours a positive energy balance by regulating glucostatic adipokines [5]. In contrast, CB1R-deficient mice have less fat than their wild-type littermates and are protected against diet-induced obesity [6,7]. Blocking the receptor with the selective CB1R antagonist rimonabant induces weight loss, increases insulin sensitivity and improves cardiovascular risk factors in overweight patients [8-11]. The mechanisms responsible for these effects remain only partially elucidated. Here, we present several lines of evidence in support of the notion that direct blockade of peripheral CB1R action in adipose tissue induces transdifferentiation in white adipocytes towards a thermogenic brown fat cell phenotype.

## Materials and Methods

Antibodies against PGC-1 $\alpha$ , pAMPK (Thr172) and AMP-activated protein kinase (AMPK) were from Cell Signaling Technology (Beverly, MA, USA). The UCP-1 and actin antibodies were purchased from Chemicon International (Temecula, CA, USA). Antibodies against  $\alpha$ 2 and PPAR $\gamma$  were from Santa Cruz Biotechnology (Santa Cruz, CA, USA). Primers for quantitative RT-PCR were ordered from Biometra (Goettingen, Germany). 8-Bromo-cAMP was purchased from Enzo Life Science GmbH (Lörrach, Germany). All other chemicals were from Sigma-Aldrich (St Louis, MO, USA), unless stated otherwise. Rimonabant was kindly provided by Sanofi-Aventis (Berlin, Germany). A 10-mM stock solution in 100% dimethyl sulfoxide (DMSO) was prepared and aliquots were stored at  $-20^{\circ}\text{C}$ . Working solutions were freshly prepared for all experiments.

## Cell Culture

Cells used in all experiments were SV40T-immortalized white or brown adipocytes generated as previously described [12,13]. Preadipocytes were cultured to confluence in Dulbecco's modified Eagle's medium (DMEM) (PAA Laboratories GmbH, Pasching, Austria), supplemented with 4.5 g/l glucose, 20 nM insulin, 1 nM T3 (Sigma-Aldrich), 20% fetal bovine serum (Invitrogen GmbH, Karlsruhe, Germany) and penicillin/streptomycin (PAA Laboratories GmbH) ('differentiation medium'). Upon attaining confluence, 500  $\mu\text{M}$  isobutylmethylxanthine, 250  $\mu\text{M}$  indomethacine and 2  $\mu\text{g}/\text{ml}$  dexamethasone (Sigma-Aldrich) were added to the differentiation medium to induce cell differentiation ('induction'). After 24 h, cells were returned to differentiation medium and cultured for 6 more days. During the entire differentiation process or as indicated, rimonabant was added in different concentrations to the medium which was changed every day.

## Small Interfering RNA

Adipocytes were transfected 3 days after induction with 200 pmol of a siRNA pool containing two different siRNAs for CB1R (Qiagen, Hilden, Germany) or with non-targeting Allstars Negative Control siRNA (Qiagen). Electroporation was performed according to the manufacturer's protocol using a Nucleofector (Amaxa AG, Cologne, Germany). In brief, the

adherent growing cells were carefully trypsinized off the plate, trypsinization was stopped by adding culture medium and cells were washed two times with phosphate-buffered saline (PBS). After centrifugation, the pellet was resuspended in 100  $\mu\text{l}$  Nucleofactor solution V (cell line Nucleofector Kit V) mixed with CB1R siRNA or control siRNA. This mixture was transferred into a cuvette and electroporation was carried out by using program T-030 for adipocytes as recommended by the manufacturer. After transfection, adipocytes were seeded on 6-well plates and further cultivated for the indicated periods of time. Forty-eight, 72 and 96 h after electroporation CB1R expression was determined. An average knock-down of 70% was achieved. Therefore, further experiments which required a stable knock-down of the CB1R were performed only during this tested time frame.

## RNA Analysis

To analyse the mRNA expression of CB1R, UCP-1 and PGC-1 $\alpha$ , quantitative real-time RT-PCR was performed with 36B4 as a housekeeping gene control. Total RNA was isolated using TRIzol reagent (Invitrogen). To optimize the RNA quality, a clean up and DNase digestion were performed using the NucleoSpin<sup>®</sup> RNA II Kit (Macherey-Nagel, Dueren, Germany). Quality of RNA was tested by photometric analysis and agarose gel electrophoresis. Two micrograms of total RNA was reverse transcribed using Superscript II (Invitrogen) and an oligo p(DT)15 primer (Roche Molecular Biochemicals, Mannheim, Germany) in the presence of RNase inhibitor (Roche Molecular Biochemicals) in a 20- $\mu\text{l}$  reaction. C-DNA was prediluted and 2  $\mu\text{l}$  was amplified in a 12- $\mu\text{l}$  PCR containing 1X SYBR<sup>®</sup> Premix Ex Taq<sup>™</sup> (TaKaRa Bio Europe, Saint-Germain-en-Laye, France) using the Mastercycler<sup>®</sup> ep realplex (Eppendorf GmbH, Hamburg, Germany). Primer sequences used were as follows: CB1R (NM\_0077726) sense TGCAGGCCTTCCTACCACTT, antisense TGTGCAGGCAGTCTGAGTCC; UCP-1 (NM\_009463) sense G TACTGGAAGCCTGGCCTTCACCTTGG, antisense ATGGTGAACCCGACAACCTTCCGAAGTG and PGC-1 $\alpha$  (NM\_008904) sense AGCACACGTTTATTCACGGGT, antisense GCCCCCAAGTCCTCACATG. PCR for all targets was performed as follows: initial denaturation at  $95^{\circ}\text{C}$  for 300 s, 40 cycles with  $95^{\circ}\text{C}$  for 20 s,  $60^{\circ}\text{C}$  for 30 s. Specific amplification was confirmed by producing melting curve profiles and by subjecting the amplification products to agarose gel electrophoresis. Relative quantification was done by using the Mastercycler<sup>®</sup> ep realplex software based on the  $\Delta\Delta\text{CT}$  method [14].

## Oil Red O Staining

Cells were washed with PBS and fixed with 10% formalin for 30 min. After removing the formalin, 5 ml of the oil red O staining solution, previously filtered (Schleicher & Schuell GmbH, Dassel, Germany), was added for 1 h. To remove excess stain and any precipitate that may have formed, the cells were rinsed several times with distilled water.

## Immunoblotting

Cells were differentiated and treated with rimonabant as indicated. After washing the cells with an ice-cold PBS, proteins were isolated using a whole-cell lysis buffer containing 10 µg/ml aprotinin and leupeptin, 2 mmol/l vanadate and phenylmethylsulphonyl fluoride. Protein content was measured based on the Bradford method using dye from Bio-Rad (Hercules, CA, USA). Proteins were separated by Sodium Dodecyl Sulfate (SDS) polyacrylamide gel electrophoresis and transferred to nitrocellulose membranes (Schleicher & Schuell). Membranes were blocked and incubated with the specific antibodies according to the manufacturer's instructions. Protein bands were visualized using chemiluminescence (Perkin Elmer GmbH, Rodgau-Jügesheim, Germany) and enhanced chemiluminescence films (Amersham Pharmacia Biotech, Freiburg, Germany). Quantification of the images was done by using Quantity One software (Bio-Rad).

## Oxygen Consumption

Respiration of adipocytes was measured by using a Clark-type oxygen electrode (Oxygraph System, Hansatech, England). Treated adipocytes were detached off the plate and rinsed with PBS. After centrifugation at 500 g for 3 min, the pellet was resuspended in DMEM without supplements. Each sample was analysed by incubating about  $10^6$  cells over a period of 15 min. Measurement was made in a magnetically stirred chamber, connected to a water circulation system to maintain a stable chamber temperature (37°C). The incoming signals were detected by software from Hansatech and converted into graphs. The rate of consumption was normalized against the number of living cells, which were stained before with trypan blue and counted in a Neubauer's counting chamber.

## Fluorescence Microscopy

Fully differentiated and rimonabant-treated adipocytes seeded in 2-well CultureSlides (Becton & Dickinson Biosciences, San Jose, CA, USA) were fixed with 4% formaldehyde. Labelling was made at room temperature for 20 min with 100 nM MitoFluorGreen, a mitochondrial-specific fluorochrome (Molecular Probes, Invitrogen), as described by the manufacturer. Images were acquired with an ApoTome fluorescence microscope (Zeiss, Goettingen, Germany).

## Flow Cytometry

Adipocytes were trypsinated, rinsed with PBS and fixed in 4% formaldehyde. After staining with MitoFluorGreen as described earlier, the fluorescence intensity of the cells was determined by a FACSCanto (Becton & Dickinson Biosciences) and analysed by the FlowJo software (Tree Star, Ashland, OR, USA).

## Cytochrome c Oxidase (COX) Activity

For cytochrome c oxidase (COX) activity measurement, we used isolated mitochondria from differentiated cells. Adipocytes were collected and resuspended in mitochondrial

buffer [0.2 mM EDTA, 0.25 M sucrose and 1% Triton-X-114 in 10 mM Tris (pH 7.8)]. Cells were ruptured using an automatic Teflon homogenizer from Schuett (Germany) and the homogenates were centrifuged at 1000 g for 10 min. Mitochondria were pelleted at 12 000 g spin for 15 min and resuspended in mitochondrial buffer supplemented with protease inhibitors (2 mM vanadate, 10 µg/ml leupeptin, 10 µg/ml aprotinin and 2 mM PMSF). Protein content was determined by the Bradford method (Bio-Rad). COX activity was determined with 20 µg of mitochondrial proteins from each treatment according to the manufacturer's protocol (Sigma). The activity was calculated from the rate of decrease in absorbance of reduced cytochrome c at 550 nm, added to the assay at a final concentration of 10 µM. No significant COX activity was detected in the 12 000 g spin supernatants.

## Electron Microscopy

Adipocytes were fixed in 2% glutaraldehyde/0.6% formaldehyde in 0.06 M sodium cacodylate/HCl buffer (pH 7.3). After postfixation in OsO<sub>4</sub>, cells were dehydrated in graded ethanol solutions and embedded in Araldite M (Fluka, Neu-Ulm, Germany). Ultrathin sections (60 nm) were prepared, stained with uranyl acetate and lead citrate and examined using a Philips EM 400T transmission electron microscope. Numbers of mitochondria were analysed by counting 50 images of each probe.

## Statistical Analysis

All results are expressed as means, and error bars depict standard errors. Unpaired student's *t*-test was performed to determine *p* values using 'sigma plot' software (SPSS Science, Chicago, IL, USA). \**p* values < 0.05 and \*\**p* values < 0.01.

## Results

### CB1 Receptor Expression is Increased after Selective CB1R Blockade

White adipocytes treated with rimonabant showed a dose- and time-dependent increase in CB1R protein as well as CB1R mRNA. Cells were incubated for 2, 4 and 8 h with 100 nM rimonabant. The highest effects were observed after 2 and 4 h with a 320% increase in CB1R mRNA (figure 1A). A similar effect was found after chronic treatment with 10 or 100 nM rimonabant for 10 days. Rimonabant was added every day during the proliferation and differentiation process. CB1R protein expression increased in a dose-dependent manner with a maximum effect at 100 nM (figure 1B).

### Cell Differentiation is Not Affected by CB1 Receptor Blockade

Selective blockade of the CB1R with rimonabant had no effect on lipid accumulation. Preadipocytes were stimulated during the proliferation and differentiation process with 100 nM rimonabant. This chronic exposure did not alter the cell morphology and lipid content (figure 2A). To confirm

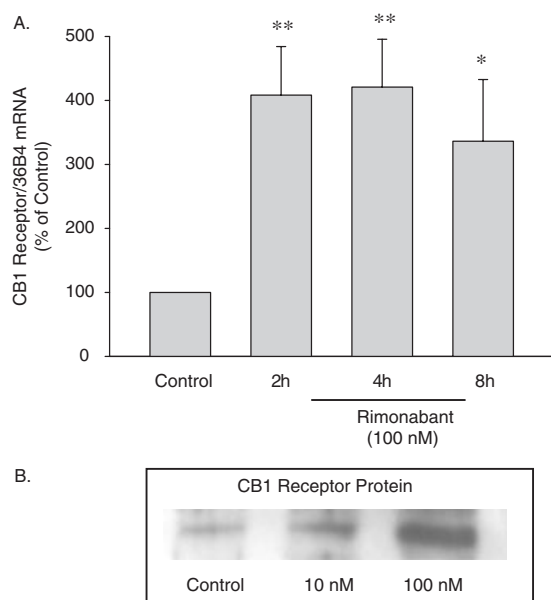


**Figure 1.** The cannabinoid receptor type 1 (CB1R) antagonist rimonabant stimulates dose and time dependently the expression of CB1R. White adipocytes were treated acute (2, 4 and 8 h; A) or chronic (everyday after seeding; B) with the selective cannabinoid CB1R antagonist rimonabant at the concentrations indicated. mRNA (A) quantification and CB1R immunoblots (B) were performed. The bar graph analysis (A) indicates a highly significant increase in CB1R mRNA expression after acute stimulation with 100 nM rimonabant for 2 and 4 h ( $n = 6$  experiments). Data were normalized using 36B4 as a housekeeping gene and expressed as percent of control. (B) Shows a representative immunoblot of the CB1R protein expression after chronic stimulation with 10 or 100 nM rimonabant. \* $p < 0.05$ , \*\* $p < 0.01$  comparing non-treated (control) to treated cells.

these findings, the expression of differentiation markers in fully differentiated cells was investigated. Neither  $\alpha P2$  nor  $PPAR\gamma$  protein expression was altered in response to chronic rimonabant treatment at 100 nM or 1  $\mu M$  concentrations as compared to non-treated controls (figure 2B).

### CB1 Receptor Blockade or Knock-down Enhances UCP-1, PGC-1 $\alpha$ and pAMPK Expression

Thermogenesis is a specific function of brown adipocytes and an important regulator of energy expenditure. We assessed UCP-1 protein expression by stimulating white adipocytes chronically with 100 nM or 1  $\mu M$  rimonabant. There was an increase in UCP-1 protein as compared to non-treated control cells. A parallel effect was seen at the RNA level. UCP-1 gene expression was measured by quantitative real-time PCR as described earlier. We found a 120% increase of UCP-1 mRNA expression after stimulating the cells with 1  $\mu M$  rimonabant (figure 3A). These results were confirmed by knock-down experiments. There was a 250% enhancement of UCP-1 mRNA expression after transfection with specific CB1R siRNA (figure 3B). This effect was not only restricted to preadipocytes undergoing differentiation but it was also seen in fully differentiated fat cells. Rimonabant administration for 8 or 24 h increased the UCP-1 expression by 120 and 160%, respectively

(figure 3C). To test the hypothesis that white adipocytes transdifferentiate into a brown phenotype, the expression of a major transdifferentiation marker was investigated. PGC-1 $\alpha$  expression was measured after chronic treatment with rimonabant for 10 days. There was a 30% increase in PGC-1 $\alpha$  mRNA expression as well as a dose-dependent enhancement in PGC-1 $\alpha$  protein amount (figure 4A). Consistent with these findings, there was also a 60% increase in PGC-1 $\alpha$  mRNA expression in response to a CB1R knock-down (figure 4B). Moreover, phosphorylation of AMPK significantly increased after chronic stimulation with 1  $\mu M$  rimonabant by 120% during the early differentiation stages (cells achieved confluence) (figure 4C).

### CB1 Receptor Blockade Promotes Mitochondrial Biogenesis

In line with the observed increase in PGC-1 $\alpha$  expression, selective CB1R blockade induced a 15% increase in mitochondrial numbers compared to non-treated cells (figure 5) as analysed on electron microscopy images. This did not appear to be associated with changes in mitochondrial size. Furthermore, mitochondria-specific fluorescent staining of white adipocytes revealed an increased signal in rimonabant-treated cells (figure 6A). There was a 70% increase in fluorescence intensity in cells treated with 1  $\mu M$  rimonabant compared to non-treated cells (figure 6C). Finally, a CB1R knock-down resulted in a 60% increase in fluorescence intensity (figure 6D).

### Rimonabant Increases Cytochrome c Oxidase Activity

COX is a large transmembrane protein complex in the mitochondrion whose activity is taken to indicate increased mitochondrial activity. Selective CB1R blockade showed a 30% increase in COX activity compared to control cells (figure 7).

### Oxygen Consumption is Increased while Blocking the CB1 Receptor

Oxygen consumption represents a final cellular read-out for increased activity of the respiratory chain. Adipocytes treated with the CB1R antagonist rimonabant, starting from day 3 of the differentiation process, increased their oxygen consumption by 40–50% compared to non-treated cells (figure 8A). To assess whether the effect of rimonabant can be mimicked by manipulating cAMP, cells were stimulated with the cAMP analog 8-Bromo-cAMP. Again, the respiration rate was increased by 25%. Similarly, knocking down the CB1R augmented oxygen consumption by 95% as compared to control cells (figure 8B).

To further characterize this effect apparently transdifferentiating white into brown adipocytes, we compared oxygen consumption of white to brown cells undergoing the same rimonabant treatment. Between brown and white non-treated control cells, there was a significant difference in oxygen consumption while this difference was abated in rimonabant-treated cells (figure 8C).

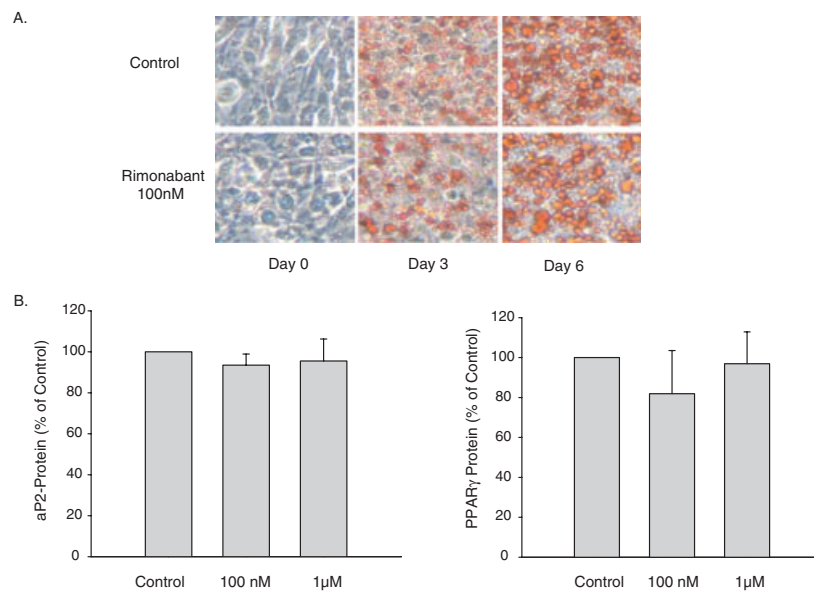


**Figure 2.** The cannabinoid receptor type 1 (CB1R) blockade has no effect on the differentiation capacity of white adipocytes. Adipocytes were chronically treated with or without rimobant and fat accumulation was visualized on day 0, 3 and 6 by oil red O staining. (A) Shows microscopic digital images, 40 times magnified. aP2 and peroxisome proliferator-activated receptor  $\gamma$  (PPAR $\gamma$ ) protein expression were measured at the end of the differentiation process by western blot analysis using specific antibodies (B). Cells were stimulated with 100 nM or 1  $\mu$ M rimobant during differentiation process. The bar graph analysis shows relative values of rimobant-treated cells referred to control cells ( $n = 3$  experiments).

## Discussion

In this study, we demonstrate the direct effects induced by the inhibition of CB1R action in adipocytes. Blockade of the CB1R action with rimobant induces thermogenic UCP-1 expression in white adipocytes accompanied by an increased mitochondrial biogenesis and insulin sensitivity. The endocannabinoid system controls energy homeostasis via both central and peripheral mechanisms [15]. The CB1R is expressed in adipose tissue and upregulated during adipogenesis [16–18]. Moreover, we demonstrated an increase of CB1R expression while treating the cells with the receptor antagonist rimobant. Interestingly, comparing our results of pharmacologic inhibition with rimobant to the knock-down of the receptor via RNA interference we found a larger effect in siRNA-transfected cells. A compensatory increase of CB1R expression after treatment of the cells with the receptor blocker rimobant may be a reason for this difference. Activation of the CB1R by its ligand results in an inhibition of the adenylate cyclase combined with a decrease of cAMP as demonstrated in several cell types [19–22]. Based on these reports, one may assume an increase of cAMP levels by rimobant treatment. In line with this reasoning, we indeed demonstrate that the effects of rimobant on oxygen consumption can be mimicked by treating the adipocytes with 8-Bromo-cAMP. In contrast to other studies, we did not find a statistically significant increase in lipid accumulation in response to chronic rimobant incubation [23,24]. This discrepancy may be explained by the different experimental approaches and model systems. Recently, we have shown that treatment of differentiated brown adipocytes with a CB1R agonist decreases UCP-1 expression [5]. The uncoupling protein is exclusively expressed by

brown adipose tissue and mediates thermogenesis [25]. UCP-1 biosynthesis is controlled at a transcriptional level during cold exposure, by retinoic acid and thyroid hormones [3]. Another major factor for UCP-1 regulation is the PGC-1 $\alpha$ . PGC-1 $\alpha$  induces the expression of genes that promote the differentiation of preadipocytes into a brown adipocyte phenotype. As a transcription factor it also participates in pathways controlling glucose homeostasis and promoting fatty acid oxidation via increasing mitochondrial function and activity [2]. After cold induction, the expression of PGC-1 $\alpha$  in brown adipocytes affects key mitochondrial proteins including ATP synthetase and the COX subunit cox II and cox IV [1], which leads to higher thermogenic activity. In this study, we demonstrate that UCP-1 as well as the PGC-1 $\alpha$  expression is significantly increased in white adipocytes in response to chronic treatment with rimobant during the differentiation process. Interestingly, this phenomenon is not restricted to preadipocytes, since we also detected an enhancement of UCP-1 in mature adipocytes treated with rimobant. Similar to the effects described for thiazolidinediones [26], CB1R inhibition induces a brown fat phenotype and may be an intriguing mechanism to mediate increases in energy expenditure [27,28]. Jbilo et al. has described an enhancement of HSP10, a major regulator of mitochondrial biogenesis, in rimobant-treated mice [29]. In line with this report, we demonstrate an increase in mitochondrial biogenesis after blocking the CB1R with rimobant or siRNA even in white adipocytes. These data are in accord with the findings of Tedesco et al., who recently reported an enhanced mitochondrial biogenesis in primary mouse adipocytes after CB1R blockade [30]. Finally, further confirmation for the notion of an increased mitochondrial activity via inhibition of CB1R action

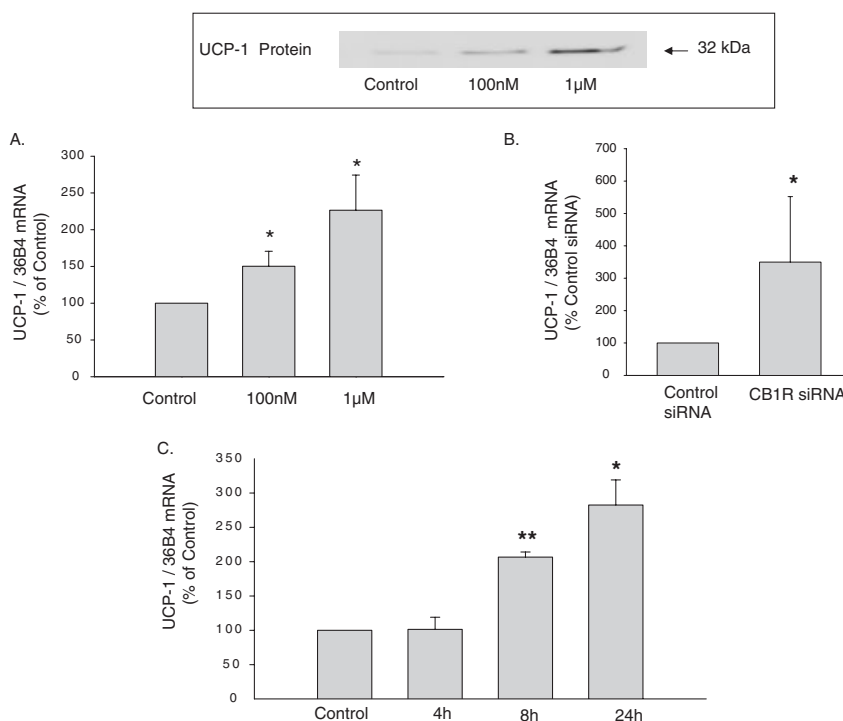


**Figure 3.** Rimonabant stimulates the uncoupling protein 1 (UCP-1) expression in white adipocytes. Cells were chronically treated with the cannabinoid receptor type 1 (CB1R) antagonist rimonabant. RNA and protein expression of the UCP-1 were analysed. A significant increase in UCP-1 expression was found on protein and RNA level after stimulation with 100 nM or 1 µM rimonabant. (A) Shows a bar graph analysis of six independent experiments. The insert in (A) shows a representative western blot analysis of the UCP-1 protein expression. A similar result was found using siRNA for CB1R knock-down (B). Seventy-two hours after CB1R siRNA transfection, the cells increased significantly the UCP-1 RNA expression. A bar graph analysis of five independent experiments is shown (B). Acute stimulation of the CB1R for 8 or 24 h enhanced the UCP-1 expression by 120 and 160%, respectively (C). A bar graph analysis of three independent experiments is shown. \*p < 0.05 in treated cells compared to control cells. All data were normalized using 36B4 as a housekeeping gene.

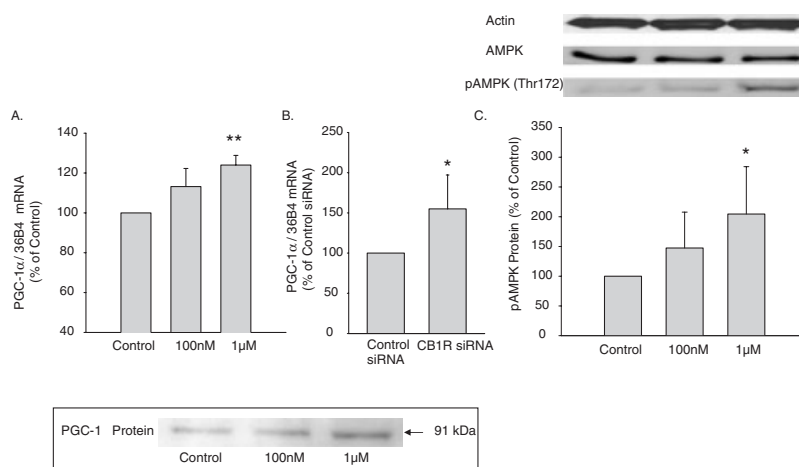


**Figure 4.** Rimonabant induces peroxisome proliferator-activated receptor γ coactivator 1α (PGC-1α) and phospho AMP-activated protein kinase (AMPK) expression. During differentiation, cells were incubated with various concentrations of rimonabant. RNA and protein lysates were prepared and quantitative RT-PCR and immunoblotting were done using a specific PGC-1α antibody. A highly significant increase was found after stimulating the adipocytes with 1 µM rimonabant. A representative immunoblot showing the band of interest and a bar graph analysis including the standard error of the mean of four independent experiments are shown (A). CB1R-specific knock-down also enhanced the PGC-1α mRNA expression. A bar graph analysis of five independent experiments is shown. Data were normalized using 36B4 as a housekeeping gene and expressed as percent of control. (B) Phosphorylation and amount of AMPK were detected by specific antibodies. A bar graph analysis of six independent experiments is shown. (C) Representative immunoblots for pAMPK, AMPK and actin as an internal control are inserted. \*p < 0.05, \*\*p < 0.01 comparing non-stimulated to rimonabant-/siRNA-treated cells.



**Figure 5.** Rimonabant increases mitochondrial biogenesis. Electron microscopy images of fully differentiated adipocytes. Mitochondria in rimonabant-treated cells are marked with pink colour, whereas the mitochondria in control cells are marked in blue.

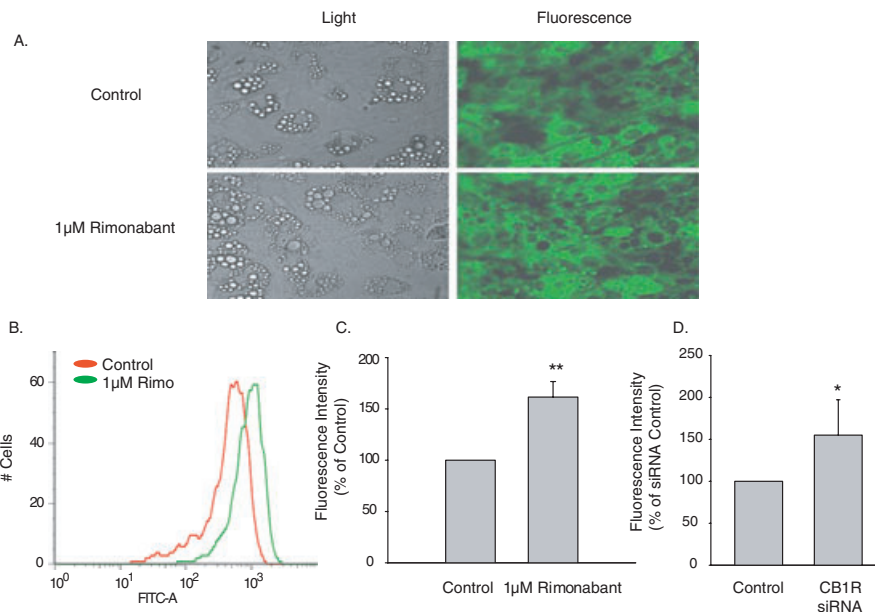


**Figure 6.** Blockade of cannabinoid receptor type 1 (CB1R) enhances mitochondrial numbers. Amount of mitochondria was detected by staining the cells with mitochondrial tracker green. Fluorescence signals were observed by fluorescence microscopy (A). Cells were analysed using fluorescence-activated cell sorting (FACS). A histogram of the FACS analysis is shown in (B). A bar graph analysis of six independent experiments is shown comparing rimonabant-treated to non-treated control cells (C). A bar graph analysis of six independent experiments using siRNA-mediated CB1R knock-down is shown (D). \* $p < 0.05$ , \*\* $p < 0.01$  comparing non-stimulated to rimonabant-/siRNA-treated cells.

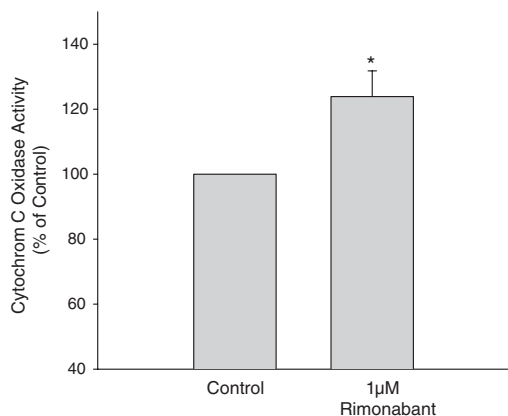


**Figure 7.** Rimonabant increases cytochrome c oxidase activity. The bar graph analysis shows relative cytochrome c oxidase activity of rimonabant-treated cells referred to control cells (n = 3 experiments). \* $p < 0.05$ .

is provided by the demonstration of augmented COX activity and increased oxygen consumption in response to selective CB1R blockade or its knock-down, respectively. We see a robust enhancement of COX activity and a highly significant increase in oxygen consumption using both experimental approaches, RNA interference and pharmacological blockade, respectively. The effect of CB1R inhibition on oxygen consumption appears relatively small. However, this small difference may contribute to a significant alteration in energy expenditure over time. Moreover, we show an increase in AMPK phosphorylation by blocking CB1R action. AMPK inhibits adipocyte lipolysis and stimulates fatty acid oxidation. Furthermore, AMPK also upregulates PGC-1 $\alpha$  expression and mitochondrial biogenesis [31]. Taken together, these findings may provide a molecular and cellular explanation for *in vivo* observations showing an enhanced basal oxygen consumption in ob/ob mice after a 7-day treatment course with rimonabant [32]. Verty et al. described a

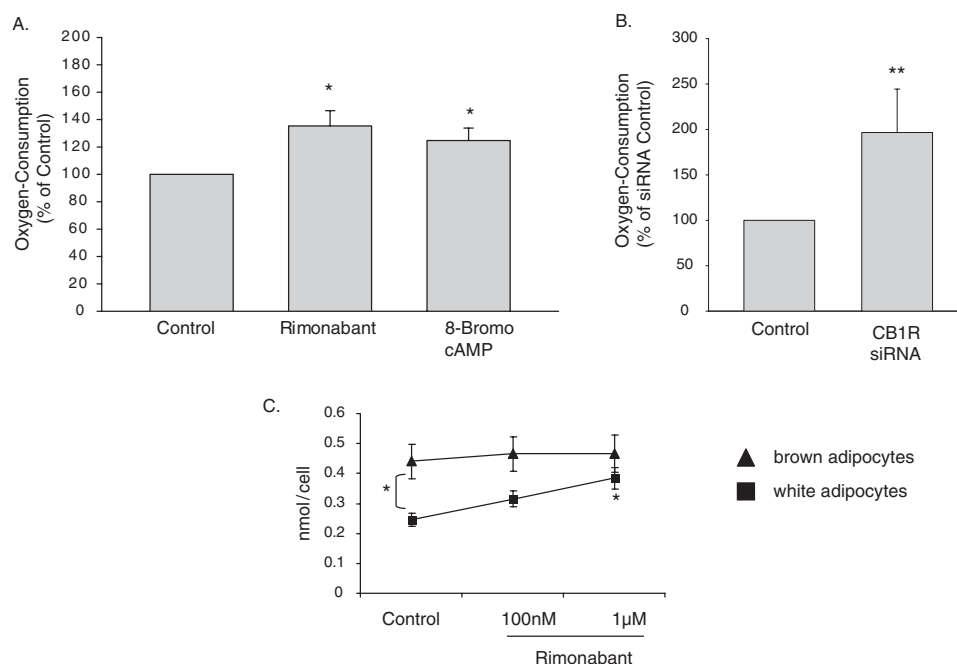


**Figure 8.** Blockade of the cannabinoid receptor type 1 (CB1R) enhances oxygen consumption in white adipocytes. Cells were treated with 1  $\mu$ M rimobant or 1 mM 8-Bromo-cAMP starting at day 3 of the differentiation process. Oxygen consumption was measured at day 6 using a Clark-type oxygen electrode. The bar graph analysis summarizes three to six independent experiments (A). A bar graph analysis of four independent experiments depicting oxygen consumption in siRNA-treated vs. non-treated control cells is shown (B). The line graph compared the respiration rate of white adipocytes to brown adipocytes (C). Three to ten independent experiments are shown. \* $p \leq 0.05$ , \*\* $p < 0.01$ .

rimonabant-induced elevation in brown adipose tissue (BAT) temperature and decreased body weight in rats, which was attenuated following denervation [28]. Our results demonstrate a direct influence of rimobant on thermogenesis in white and brown adipocytes. This may provide a partial molecular basis for these findings. However, one must assume that the direct effects are not the exclusive mechanism of rimobant action on energy expenditure.

Motaghedi et al. describe an enhanced glucose uptake in adipocytes [33]. Interestingly, we found a marginal but a significant increase in insulin-induced glucose uptake after chronic rimobant treatment of white adipocytes (data not shown). We cannot explain this discrepancy but different methodic approaches as well as a different cell system may be a possible explanation. Interestingly, in the other major peripheral insulin sensitive tissue, that is skeletal muscle, a recent paper reports enhanced insulin sensitivity by rimobant treatment, similar to our findings. Esposito et al. find an increase in insulin-induced glucose uptake in skeletal muscle cells [34]. In line with our findings on the transdifferentiation of white adipocytes into a brown fat phenotype, enhancing the glucose uptake might represent a cellular mechanism to increase fuel provision for enhanced mitochondrial activity.

In summary, our data present direct evidence for the induction of a brown fat phenotype in white adipocytes via inhibition of CB1R action. These effects may explain findings from experimental and clinical studies postulating peripheral weight loss-inducing effects of the CB1R antagonist rimobant.

## Acknowledgements

We would like to thank J. Eндler for her technical assistance with electron microscopy. This study was supported by a translational research grant from Sanofi-Aventis, Germany and a grant from the Deutsche Forschungsgemeinschaft (DFG) to J. K.: (KL 1131/4-1).

## References

- Puigserver P, Wu Z, Park CW, Graves R, Wright M, Spiegelman BM. A cold-inducible coactivator of nuclear receptors linked to adaptive thermogenesis. *Cell* 1998; **92**: 829–839
- Medina-Gomez G, Gray S, Vidal-Puig A. Adipogenesis and lipotoxicity: role of peroxisome proliferator-activated receptor gamma (PPARgamma) and PPARgamma-macrocovactor-1 (PGC1). *Public Health Nutr* 2007; **10**: 1132–1137.
- Tiraby C, Tavernier G, Lefort C et al. Acquisition of brown fat cell features by human white adipocytes. *J Biol Chem* 2003; **278**: 33370–33376.
- Pagotto U, Vicennati V, Pasquali R. The endocannabinoid system and the treatment of obesity. *Ann Med* 2005; **37**: 270–275.
- Perwitz N, Fasshauer M, Klein J. Cannabinoid receptor signaling directly inhibits thermogenesis and alters expression of adiponectin and visfatin. *Horm Metab Res* 2006; **38**: 356–358.
- Cota D, Marsicano G, Tschop M et al. The endogenous cannabinoid system affects energy balance via central orexigenic drive and peripheral lipogenesis. *J Clin Invest* 2003; **112**: 423–431.
- Ravinet Trillou C, Delgorge C, Menet C, Arnone M, Soubrie P. CB1 cannabinoid receptor knockout in mice leads to leanness, resistance to diet-induced obesity and enhanced leptin sensitivity. *Int J Obes Relat Metab Disord* 2004; **28**: 640–648.

8. Van Gaal LF, Rissanen AM, Scheen AJ, Ziegler O, Rossner S. Effects of the cannabinoid-1 receptor blocker rimonabant on weight reduction and cardiovascular risk factors in overweight patients: 1-year experience from the RIO-Europe study. *Lancet* 2005; **365**: 1389–1397.
9. Despres JP, Golay A, Sjoström L. Effects of rimonabant on metabolic risk factors in overweight patients with dyslipidemia. *N Engl J Med* 2005; **353**: 2121–2134.
10. Pi-Sunyer FX, Aronne LJ, Heshmati HM, Devin J, Rosenstock J. Effect of rimonabant, a cannabinoid-1 receptor blocker, on weight and cardiometabolic risk factors in overweight or obese patients: RIO-North America: a randomized controlled trial. *JAMA* 2006; **295**: 761–775.
11. Scheen AJ, Finer N, Hollander P, Jensen MD, Van Gaal LF. Efficacy and tolerability of rimonabant in overweight or obese patients with type 2 diabetes: a randomised controlled study. *Lancet* 2006; **368**: 1660–1672.
12. Fasshauer M, Klein J, Kriaciunas KM, Ueki K, Benito M, Kahn CR. Essential role of insulin receptor substrate 1 in differentiation of brown adipocytes. *Mol Cell Biol* 2001; **21**: 319–329.
13. Klein J, Fasshauer M, Klein HH, Benito M, Kahn CR. Novel adipocyte lines from brown fat: a model system for the study of differentiation, energy metabolism, and insulin action. *Bioessays* 2002; **24**: 382–388.
14. Pfaffl MW, Horgan GW, Dempfle L. Relative expression software tool (REST) for group-wise comparison and statistical analysis of relative expression results in real-time PCR. *Nucleic Acids Res* 2002; **30**: e36.
15. Di Marzo V, Matias I. Endocannabinoid control of food intake and energy balance. *Nat Neurosci* 2005; **8**: 585–589.
16. Pagano C, Pilon C, Calcagno A et al. The endogenous cannabinoid system stimulates glucose uptake in human fat cells via phosphatidylinositol 3-kinase and calcium-dependent mechanisms. *J Clin Endocrinol Metab* 2007; **92**: 4810–4819.
17. Roche R, Hoareau L, Bes-Houtmann S et al. Presence of the cannabinoid receptors, CB1 and CB2, in human omental and subcutaneous adipocytes. *Histochem Cell Biol* 2006; **126**: 177–187.
18. Spoto B, Fezza F, Parlongo G et al. Human adipose tissue binds and metabolizes the endocannabinoids anandamide and 2-arachidonoylglycerol. *Biochimie* 2006; **88**: 1889–1897.
19. Howlett AC. Inhibition of neuroblastoma adenylate cyclase by cannabinoid and nantradol compounds. *Life Sci* 1984; **35**: 1803–1810.
20. Bayewitch M, Avidor-Reiss T, Levy R, Barg J, Mechoulam R, Vogel Z. The peripheral cannabinoid receptor: adenylate cyclase inhibition and G protein coupling. *FEBS Lett* 1995; **375**: 143–147.
21. Felder CC, Joyce KE, Briley EM et al. Comparison of the pharmacology and signal transduction of the human cannabinoid CB1 and CB2 receptors. *Mol Pharmacol* 1995; **48**: 443–450.
22. Pacheco MA, Ward SJ, Childers SR. Identification of cannabinoid receptors in cultures of rat cerebellar granule cells. *Brain Res* 1993; **603**: 102–110.
23. Bellocchio L, Cervino C, Vicennati V, Pasquali R, Pagotto U. Cannabinoid type 1 receptor: another arrow in the adipocytes' bow. *J Neuroendocrinol* 2008; **20**(Suppl. 1): 130–138.
24. Gary-Bobo M, Elachouri G, Scatton B, Le Fur G, Oury-Donat F, Bensaid M. The cannabinoid CB1 receptor antagonist rimonabant (SR141716) inhibits cell proliferation and increases markers of adipocyte maturation in cultured mouse 3T3 F442A preadipocytes. *Mol Pharmacol* 2006; **69**: 471–478.
25. Nicholls DG, Rial E. A history of the first uncoupling protein, UCP1. *J Bioenerg Biomembr* 1999; **31**: 399–406.
26. Wilson-Fritch L, Burkart A, Bell G et al. Mitochondrial biogenesis and remodeling during adipogenesis and in response to the insulin sensitizer rosiglitazone. *Mol Cell Biol* 2003; **23**: 1085–1094.
27. Herling AW, Kilp S, Elvert R, Haschke G, Kramer W. Increased energy expenditure contributes more to the body weight-reducing effect of rimonabant than reduced food intake in candy-fed wistar rats. *Endocrinology* 2008; **149**: 2557–2566.
28. Verty AN, Allen AM, Oldfield BJ. The effects of rimonabant on brown adipose tissue in rat: implications for energy expenditure. *Obesity (Silver Spring)* 2009; **17**: 254–261.
29. Jbilo O, Ravinet-Trillou C, Arnone M et al. The CB1 receptor antagonist rimonabant reverses the diet-induced obesity phenotype through the regulation of lipolysis and energy balance. *FASEB J* 2005; **19**: 1567–1569.
30. Tedesco L, Valerio A, Cervino C et al. Cannabinoid type 1 receptor blockade promotes mitochondrial biogenesis through endothelial nitric oxide synthase expression in white adipocytes. *Diabetes* 2008; **57**: 2028–2036.
31. Towler MC, Hardie DG. AMP-activated protein kinase in metabolic control and insulin signaling. *Circ Res* 2007; **100**: 328–341.
32. Liu YL, Connoley IP, Wilson CA, Stock MJ. Effects of the cannabinoid CB1 receptor antagonist SR141716 on oxygen consumption and soleus muscle glucose uptake in Lep(ob)/Lep(ob) mice. *Int J Obes (Lond)* 2005; **29**: 183–187.
33. Motaghedi R, McGraw TE. The CB1 endocannabinoid system modulates adipocyte insulin sensitivity. *Obesity (Silver Spring)*. 2008; **16**: 1727–1734.
34. Esposito I, Proto MC, Gazzero P et al. The cannabinoid CB1 receptor antagonist rimonabant stimulates 2-deoxyglucose uptake in skeletal muscle cells by regulating the expression of phosphatidylinositol-3-kinase. *Mol Pharmacol* 2008; **74**: 1678–1686.